

Synthesis and Characterization of Polyaniline-Multiwalled Carbon Nanotube Nanocomposites and Its Electrical Percolation Behavior

S. G. Bachhav, D. R. Patil*

Nanomaterial Research Laboratory, R.C. Patel Arts, Commerce & Science College, Shirpur, India

Abstract The nanocomposites of polyaniline (PANI) and carboxylated multi-walled carbon nanotubes (MWCNTs) were synthesized by in situ chemical oxidative polymerization method using HCl as a dopant and Ammonium persulphate (APS) as an oxidant. The MWCNTs were carboxylic functionalized and were ultrasonicated to obtain uniform dispersion within the PANI matrix. Field emission scanning electron microscopy (FE-SEM) was used to characterize the morphology of the nanocomposites. X-Ray diffraction (XRD), Fourier Transform Infrared (FT-IR) spectroscopy, Raman spectroscopy and UV-Vis spectroscopy were used to characterize the synthesized PANI-MWCNT nanocomposites. It was found that in situ polymerized PANI layer matrix was formed on carboxylated MWCNT and there was uniform dispersion of MWCNTs within the PANI matrix with significant interaction between PANI and MWCNTs. The electrical conductivity of composites at room temperature was measured and their percolation threshold briefly discussed.

Keywords Polyaniline, Carbon nanotubes, in situ polymerization, Electrical conductivity

1. Introduction

A polymer-Carbon nanotubes (CNTs) composite is a combination of polymer matrix with CNTs that possess properties that are unique and cannot be obtained with each material acting alone. CNTs with unique electrical, thermal and mechanical properties has become a potential candidate for wide range of applications in nanoscience and nanotechnology, suitable to serve as conducting filler in polymer nanocomposites. As carbonaceous nanofillers, CNTs play a very promising role due to their better structural and functional properties such as high aspect ratio, high mechanical strength, and high electrical properties etc. than other fillers [1].

The conducting polymers receive much attention because of their wide application range. Among the several conducting polymers, Polyaniline (PANI) has been studied extensively due to its high electrical conductivity, abundant raw materials, easy synthesis, good environmental stability, cost effectiveness and simple redox chemistry [2]. The PANI-CNT nanocomposites is one of the versatile nanocomposites due to the numerous applications such as Gas sensor [3, 4], Biosensor [5], Supercapacitor [6], Solar cell [7], Fuel cell [8], Corrosion protection [9], etc. Out of

several synthesis methods of PANI-CNT nanocomposites reported in literature, in situ polymerization is the most used synthesis method as it enables grafting of polymer molecules on CNT, which leads to the better dispersion coefficient and better interaction between CNT and polymer matrix. Incorporating CNT as fillers into PANI enhance the conductivity of PANI nanocomposites as CNT could have much higher electrical conductivity than PANI. The CNT could behave as conducting bridge between conducting domains of PANI thus enhanced the electrical conductivity of PANI [10].

The effect of the functionalized multi-walled carbon nanotubes (f-MWCNTs) content on the conductivity of PANI-MWCNT composites was studied by many researchers [11, 12]. For low fractions of CNT, the conductivity is mainly determined by the PANI as it is the main constituent. The conductivity of PANI Emeraldine Salt based composites usually increases with CNT content [13, 14]. When an adequate amount of filler is loaded, a "percolation" path of connected fillers forms and allows charge transport through the material. At this critical concentration, called the percolation threshold, the conductivity rapidly increases.

In the present work, we report the synthesis of PANI-MWCNT nanocomposites by in situ polymerization. MWCNTs can be covalently functionalized to well disperse and to enable grafting surface. This work was aimed to obtained good dispersion of MWCNTs within PANI matrix to achieve enhancement in electrical properties of the

* Corresponding author:

dr.drpatil@gmail.com (D. R. Patil)

Published online at <http://journal.sapub.org/materials>

Copyright © 2015 Scientific & Academic Publishing. All Rights Reserved

nanocomposites. The percolation behaviour of synthesized nanocomposites was also discussed.

2. Experimental

2.1. Materials

MWCNTs and Triton X-100 used were received from sigma Aldrich. The aniline monomer used was acquired from Rankem (Mumbai). Ammonium persulphate (APS) was used as oxidizing agents acquired from SDFC (Mumbai). All these reagents used were analytical grade.

2.2. Functionalization of MWCNT

Surface modification and functionalization of MWCNTs were made by using acid boiling reflux treatment. For this, MWCNTs (0.5 g) were suspended in H_2SO_4 and HNO_3 in a ratio of 3:1v/v to introduce the carboxylic group into the surface of MWCNTs. The suspension was refluxed with vigorous stirring at $80^\circ C$ for 12 h. After cooling to the room temperature, the mixture was filtered with filter paper. The filtrated solid was then washed thoroughly with DI water until neutral pH, and then washed with ethanol. The collected product was dried in oven at $60^\circ C$ for 12 h. This product is referred to as functionalized MWCNTs [15].

2.3. Synthesis of PANI-MWCNT Nanocomposites

The PANI-MWCNT nanocomposites were synthesized by in situ chemical oxidative polymerization. In a typical synthesis experiment, the desired quantity of functionalized MWCNTs was added to 60 ml distilled water. A certain amount of Triton X-100 was added as a surfactant to this mixture so as to disperse the MWCNTs in water. The solution then ultrasonicated over 1 h to form well dispersed MWCNT solution. The 2 ml of aniline monomer was added into this MWCNT solution with constant stirring. After addition of aniline to MWCNT solution, the mixture was again sonicated for 10 min. The 60 ml of 1M HCl was prepared and added to the Aniline-MWCNT solution. The 0.35M APS solution was prepared by dissolving required amount of APS into 60 ml distilled water and was added drop wise to Aniline-MWCNT-HCl mixture solution for 30 min with constant stirring. The stirring was continued for 4 h and then kept standing for overnight to obtained polymerized dark-green precipitate. The polymerized solution was then filtered and washed several times with distilled water until the filtrate became acid free, and then washed with acetone, ethanol and methanol. The precipitate was dried in an oven at $60^\circ C$ for 12 h to obtain PANI-MWCNT nanocomposite.

The six PANI-MWCNT nanocomposite samples were prepared for different amount of functionalized MWCNTs such as 5 mg, 10 mg, 20 mg, 40 mg, 80 mg and 160 mg keeping PANI concentration constant. The % content of MWCNT in PANI matrix was 0.25%, 0.50%, 1%, 2%, 4% and 8%. The pristine PANI sample was also synthesized

using the similar method given above except use of MWCNTs.

2.4. Characterization

The morphology of the synthesized nanocomposites was studied on Hitachi S4800 Type-II Field Emission Scanning Electron Microscopy (FESEM). X-ray diffraction (XRD) patterns were performed on a Bruker D8 Advance diffractometer with $Cu K\alpha$ radiation. Raman spectra were recorded at room temperature on JY Horiba HR800 Raman spectrometer employing 488 nm Argon laser beam. Fourier transform infrared (FT-IR) spectra were recorded on a Shimadzu IR Affinity spectrophotometer with KBr pellets to ensure functional groups. UV-Vis spectra were recorded on Shimadzu UV-2450 spectrophotometer using quartz cell.

2.5. Conductivity Measurement

The conductivity of as synthesized composites at room temperature were determined by making the pellets of 15 mm diameter by motorized hydraulic press under identical conditions such as pressure, temperature, time etc. The silver paste contact was made on both sides of pellet and bulk resistance was measured by Keithley 2000 multimeter. The dc conductivity was then determined using the measured resistance and thickness of pellet.

3. Result and Discussion

3.1. Characterization of PANI-MWCNT Nanocomposite

The FESEM images of pure PANI, PANI-MWCNT and functionalized MWCNTs were shown in Figure 1. The intermingle ropes with smooth surface of functionalized MWCNTs with diameter about 10 nm and lengths up to few μm was observed as shown in Figure 1(a). The pure PANI granular structure with average diameter about 100 nm is observed in the image shown in Figure 1(b). The nanocomposites obtained by grafting PANI on surface of MWCNTs producing thick layer PANI on MWCNT resulted in elongated granular form with diameter in the range of 100-150 nm for 4 wt. % MWCNT loading as observed in Figure 1(c). The same structure with average diameter of 15-20 nm was observed for higher loading of MWCNTs (8 wt%), which revealed that thin layer of PANI deposited on surface of MWCNTs as shown in Figure 1(d).

The XRD pattern of PANI, PANI-MWCNT nanocomposites and MWCNTs were represented in Figure 2. The spectra MWCNTs show the peaks at $2\theta = 26^\circ$ and 43° can be attributed to graphite like structure (002) and (100) respectively. The XRD patterns of the pure PANI and all nanocomposites samples show that the peaks are scattered at 2θ values between 10° and 30° , where the crystalline peaks noticed at $2\theta = \sim 15^\circ, 20^\circ, 25^\circ$ and 27° representing (011), (020),(200) and (121) of doped PANI salt [11]. The intense peak centred at $2\theta = 25^\circ$ could be attributed to periodicity perpendicular to the polymer chain, which is similar to that acid doped PANI. This result demonstrate

that the carboxylated MWCNT doped PANI is partial crystalline polymer. The peak intensities are found to be increased with increase in the content of MWCNT in the nanocomposites. This indicates that the periodicity becomes regular with increasing MWCNTs contents. The formation of PANI-MWCNT nanocomposites was due to π - π interaction between MWCNT and PANI [16]. The diffraction peaks of MWCNT overlapped with PANI after complete in situ polymerization process.

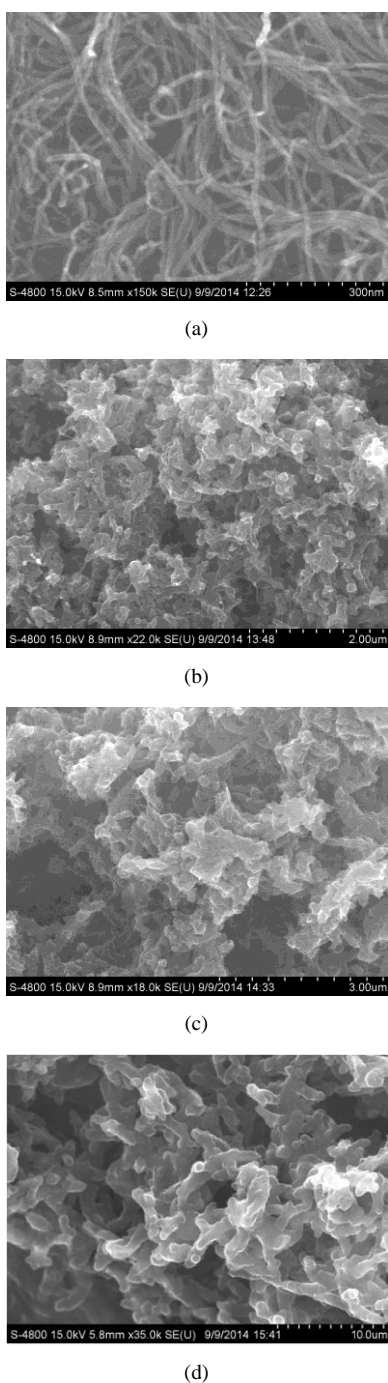


Figure 1. FE-SEM images of (a) f-MWCNT (b) PANI and PANI-MWCNT nanocomposites at MWCNTs contents of (c) 4 wt.% and (d) 8 wt.%

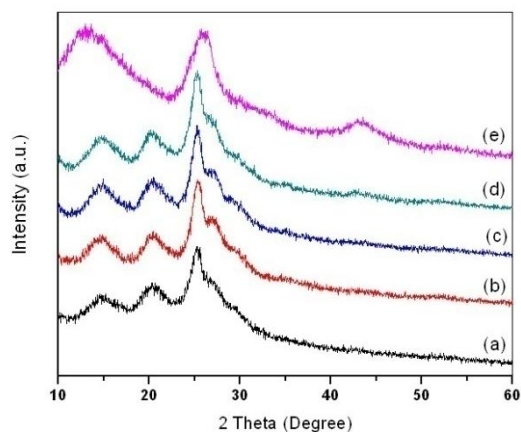


Figure 2. XRD patterns of (a) PANI, PANI-MWCNT nanocomposites at MWCNT contents of (b) 0.5 wt.%; (c) 4 wt.%; (d) 8 wt.%; (e) f-MWCNT

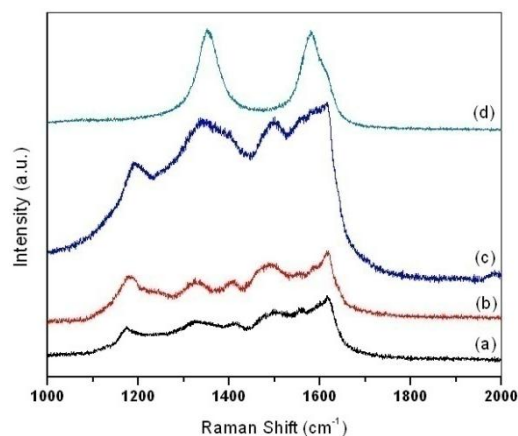


Figure 3. Raman spectroscopy of (a) pure PANI, PANI-MWCNT nanocomposites at MWCNTs contents of (b) 4 wt.%; (c) 8 wt.% and (d) MWCNT

Raman spectroscopy was carried out to ensure the interaction between PANI and MWCNTs. Figure 3 show the Raman spectra Pure PANI, MWCNT and PANI-MWCNT nanocomposites. The Raman spectrum of the carboxylated MWCNTs demonstrated two prominent characteristics peaks: D band (1350 cm^{-1}) and G band (1580 cm^{-1}). The D band represents a disorder induced feature and is usually due to presence of amorphous disordered carbon structure of CNTs [17] and G band represents stretching mode of C-C bond [18]. In the spectrum of pure PANI, the two characteristics peaks appeared at 1170 and 1494 cm^{-1} , which are assigned to C-H bending in benzenoid structure and C=N stretching in quinoid structure. The broad peak appeared at 1325 cm^{-1} is assigned to the stretching mode of C-N^{*+} delocalized polaronic structure, which is characteristics of the protonated imine form of polyaniline [16]. The peak at 1615 cm^{-1} is associated to the C-C stretching of the benzenoid structure [19]. The band at 1325 cm^{-1} corresponding to C-N^{*+} stretching band is shifted to higher wavenumber for PANI-MWCNT nanocomposites. This shifting could be ascribed to electrostatic interaction

between the C- N⁺ species of PANI matrix and the COO-species of the MWCNTs [20]. Also, in the Raman spectra of synthesized nanocomposites, the intensity of C-N⁺ stretching band at ~1330 cm⁻¹ increased, which is representation of the induced chemical doping of PANI backbone by MWCNTs. The increase in relative intensity of Raman bands of PANI-MWCNTs nanocomposites at ~1620 cm⁻¹ and to at ~1330 cm⁻¹ could be attributed to formation of more conductive PANI matrix with rich polaronic structure or the strong interaction between the MWCNTs and conjugated PANI backbone, which facilitate the electron delocalization [21].

The FT-IR spectra recorded for MWCNT, PANI and its nanocomposites in the 400-4000 cm⁻¹ range is shown in Figure 4. In the FT-IR spectrum of functionalized MWCNT, the peaks at 1390 and 1535 cm⁻¹ attributed to bending vibration of O-H group and carbonyl, respectively. The small intense peak at ~1700 corresponded to the C=O stretching vibration mode, representing the formation of the carboxylic groups and a broad peak at 3460 cm⁻¹ characteristic of an O-H stretch was observed due to alcoholic or phenolic carboxylic groups. These results specified that the MWCNTs had been successfully oxidized into carboxylated carbon nanotubes [22]. For pure PANI, the characteristics peaks at 1572 and 1476 cm⁻¹ are assigned to the C=C stretching of quinoid rings and benzenoid rings, respectively. The characteristics peaks at 1290 and 1105 cm⁻¹ are attributed to the C-N stretching vibration of the secondary aromatic amine group and aromatic C-H in plane bending vibration respectively [23]. The peak at 795 cm⁻¹ represent C-H out of plane bending vibration, while the small peak at 870 cm⁻¹ represent para-distributed aromatic rings indicating polymer formation [24]. The peak at 1232 cm⁻¹ is owing to conducting form of polyaniline indicating that the polyaniline exist in conducting emeraldine form [25]. When the composite of PANI with MWCNT form, no new absorption peaks observed, giving identical spectra as of PANI [26]. It was observed that the peak intensity decreased in the spectra of PANI-MWCNT nanocomposites indicating the strong interaction between PANI chain and the surface of MWCNTs. The decrease in intensity can be due to the fact that the PANI content decreased, when the MWCNT content increased. Thus the FT-IR measurements ensure the formation of PANI on the wall of MWCNTs by in situ chemical polymerization process [27].

To understand the effect of addition of MWCNTs in PANI matrix, the UV-vis spectroscopy was carried out. Figure 5 depicts the UV-vis spectra of pure PANI, PANI-MWCNT nanocomposites and MWCNTs. UV-vis spectrum of PANI exhibited characteristic absorption bands at 350, 450 and 860 nm [23]. These absorption peaks were also appeared in the spectrum of the PANI-MWCNT nanocomposites, where the presence of small peak at ~350 nm attributed to $\pi \rightarrow \pi^*$ transition of the benzenoid rings, while the shoulder at ~450 nm represents polaronic peak representing the protonation of the polymer and the peak at ~860 nm showing free carrier tail, confirm the presence of

conducting emeraldine salt phase of the polymer [24]. There is no absorption in the 300-800 nm range for MWCNT sample as reported by T,-M Wu et al. [28].

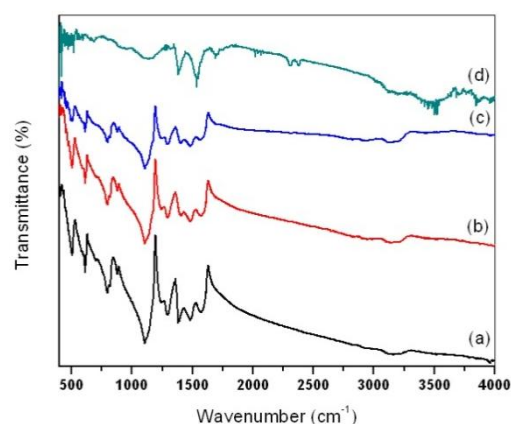


Figure 4. FT-IR spectrum of (a) pure PANI, PANI-MWCNT nanocomposites at MWCNTs contents of (b) 2 wt. %; (c) 8 wt. % and (d) MWCNT

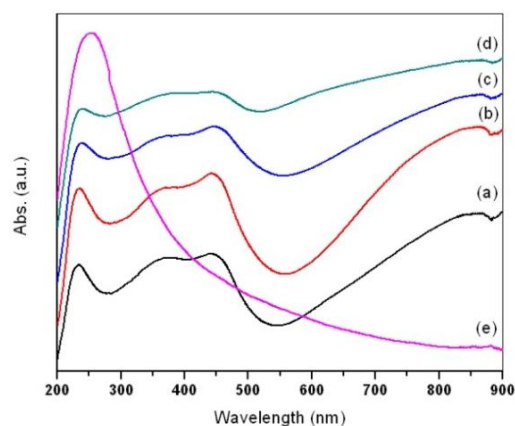


Figure 5. UV-Visible spectra of (a) pure PANI, PANI-MWCNT nanocomposites at different MWCNTs contents of (b) 0.5 wt %; (c) 1 wt %; (d) 4 wt %; (e) MWCNT

3.2. Electrical Conductivity

The curve of dc conductivity at room temperature against MWCNT contents is shown in Figure 6. It was found that conductivity was lowest for pure PANI and increased with content of MWCNT [29]. It was increased slowly for up to 1% MWCNT content but increased rapidly after 1wt% MWCNT content. The lowest conductivity obtained for pure PANI is 0.17 S/cm and increased from the value 0.22 S/cm to 3.32 S/cm for PANI-MWCNT composites having MWCNT concentration range of 0.25% to 8%. This represents an increase of conductivity nearly twenty times of magnitude as compared with pure PANI, which may be attributed to the synergistic effect between PANI and MWCNT in forming interpenetrating conductive network. The lower conductivity at low filler concentration is due the fact that excessive PANI formed aggregation over the surface MWCNTs, consequently conductive channels formed by MWCNTs are separated from each other. This

prevented the transport of effective charge along the conductive network [30] and the conductivity of PANI-MWCNT nanocomposites are contributed by pristine PANI only [31].

As the concentration of MWCNT fillers increased, they come into contact with each other to form a three dimensional conductive network where the long range connectivity and conductivity are suddenly established [32]. The concentration of conductive fillers at which this transition occurs is known to as the percolation threshold.

According to classical percolation theory, the conductivity of composite materials can be expressed by the scaling law as the conductive filler content increases [33]:

$$\sigma_c = A(\rho - \rho_c)^t \quad (1)$$

Where σ_c represents the electrical conductivity of the nanocomposite, A is a constant, ρ_c the percolation threshold, ρ the filler mass fraction, and t the critical exponent for the conductivity. The expression given in Equation (1) is valid for both insulating as well as conductive matrices incorporated with highly conductive fillers. The above equation clearly indicates that as the filler mass fraction increases beyond the percolation threshold, the composite conductivity increases sharply as conductive network paths begin to establish. It can observe that for as synthesized nanocomposites, the percolation threshold occurs at 1 wt % MWCNT content.

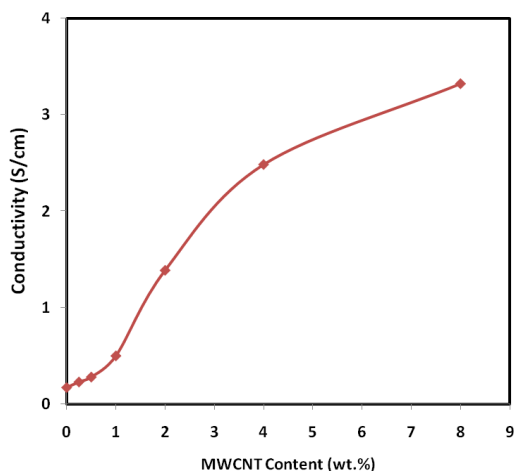


Figure 6. Room temperature electrical conductivity of PANI-MWCNT nanocomposites versus the weight percentage of MWCNT

The filler content is not only the parameter to determine the electrical conductivity of the composite, but the filler aspect ratio is another important conductivity dependent parameter. The conducting fillers such as MWCNTs with high aspect ratio are more effective in forming conductive network and produce a low percolation threshold [34, 35].

4. Conclusions

A PANI-MWCNT nanocomposites has been successfully synthesized by in situ oxidation polymerization of aniline

monomer in the presence of MWCNT with different content. FE-SEM images confirm that PANI has successfully formed on the surface of MWCNTs. XRD, Raman, FT-IR and UV-vis spectra revealed the incorporation of MWCNT into the PANI matrix. The significant enhancement in conductivity is observed with increasing MWCNT weight percentage and is indicative of percolative character. The percolation threshold of conductivity was occurred at 1 wt % MWCNT content for synthesized PANI-MWCNT nanocomposites.

ACKNOWLEDGMENTS

The authors are grateful to University Grant Commission (UGC), New Delhi for financial support through minor research project scheme no. F. 47-809/13 (WRO). The authors are also thankful to UGC-DAE Consortium for Scientific Research centre, Indore for providing the characterization facilities and the management of R.C. Patel Educational trust for their continuous encouragement and support.

REFERENCES

- [1] G. Mittal, V. Dhand, K. Y. Rhee, S.-J. Park, and W. R. Lee, "A review on carbon nanotubes and graphene as fillers in reinforced polymer nanocomposites," *Journal of Industrial and Engineering Chemistry*, vol. 21, pp. 11-25, 2015.
- [2] S. Palaniappan and A. John, "Polyaniline materials by emulsion polymerization pathway," *Progress in Polymer Science*, vol. 33, pp. 732-758, 2008.
- [3] W. K. Jang, J. Yun, H.-I. Kim, and Y.-S. Lee, "Preparation and characteristics of conducting polymer-coated multiwalled carbon nanotubes for a gas sensor," *Carbon letters*, vol. 12, pp. 162-166, 2011.
- [4] J. Yun, J. S. Im, H.-I. Kim, and Y.-S. Lee, "Effect of oxyfluorination on gas sensing behavior of polyaniline-coated multi-walled carbon nanotubes," *Applied Surface Science*, vol. 258, pp. 3462-3468, 2012.
- [5] T. H. Le, N. T. Trinh, L. H. Nguyen, H. B. Nguyen, V. A. Nguyen, and T. D. Nguyen, "Electrosynthesis of polyaniline-multiwalled carbon nanotube nanocomposite films in the presence of sodium dodecyl sulfate for glucose biosensing," *Advances in Natural Sciences: Nanoscience and Nanotechnology*, vol. 4, p. 025014, 2013.
- [6] M. S. Dorraji, I. Ahadzadeh, and M. Rasoulifard, "Chitosan/polyaniline/MWCNT nanocomposite fibers as an electrode material for electrical double layer capacitors," *International Journal of Hydrogen Energy*, vol. 39, pp. 9350-9355, 2014.
- [7] H. Zhang, B. He, Q. Tang, and L. Yu, "Bifacial dye-sensitized solar cells from covalent-bonded polyaniline-multiwalled carbon nanotube complex counter electrodes," *Journal of Power Sources*, vol. 275, pp. 489-497, 2015.

- [8] H.-F. Cui, L. Du, P.-B. Guo, B. Zhu, and J. H. Luong, "Controlled modification of carbon nanotubes and polyaniline on macroporous graphite felt for high-performance microbial fuel cell anode," *Journal of Power Sources*, vol. 283, pp. 46-53, 2015.
- [9] A. M. Kumar and Z. M. Gasem, "In situ electrochemical synthesis of polyaniline/f-MWCNT nanocomposite coatings on mild steel for corrosion protection in 3.5% NaCl solution," *Progress in Organic Coatings*, vol. 78, pp. 387-394, 2015.
- [10] C. Oueiny, S. Berlioz, and F.-X. Perrin, "Carbon nanotube – polyaniline composites," *Progress in Polymer Science*, vol. 39, pp. 707-748, 2014.
- [11] T.-M. Wu and Y.-W. Lin, "Doped polyaniline/multi-walled carbon nanotube composites: Preparation, characterization and properties," *Polymer*, vol. 47, pp. 3576-3582, 2006.
- [12] Z. Morávková, M. Trchová, E. Tomšík, J. Čechvala, and J. Stejskal, "Enhanced thermal stability of multi-walled carbon nanotubes after coating with polyaniline salt," *Polymer Degradation and Stability*, vol. 97, pp. 1405-1414, 2012.
- [13] M. Trchová, E. N. Konyushenko, J. Stejskal, J. Kovářová, and G. Ćirić-Marjanović, "The conversion of polyaniline nanotubes to nitrogen-containing carbon nanotubes and their comparison with multi-walled carbon nanotubes," *Polymer Degradation and Stability*, vol. 94, pp. 929-938, 2009.
- [14] T.-M. Wu, Y.-W. Lin, and C.-S. Liao, "Preparation and characterization of polyaniline/multi-walled carbon nanotube composites," *Carbon*, vol. 43, pp. 734-740, 2005.
- [15] C. L. Ngo, Q. T. Le, T. T. Ngo, D. N. Nguyen, and M. T. Vu, "Surface modification and functionalization of carbon nanotube with some organic compounds," *Advances in Natural Sciences: Nanoscience and Nanotechnology*, vol. 4, p. 035017, 2013.
- [16] P. Kar and A. Choudhury, "Carboxylic acid functionalized multi-walled carbon nanotube doped polyaniline for chloroform sensors," *Sensors and Actuators B: Chemical*, vol. 183, pp. 25-33, 2013.
- [17] M. S. Dresselhaus, G. Dresselhaus, R. Saito, and A. Jorio, "Raman spectroscopy of carbon nanotubes," *Physics reports*, vol. 409, pp. 47-99, 2005.
- [18] M. Cochet, G. Louarn, S. Quillard, J. Buisson, and S. Lefrant, "Theoretical and experimental vibrational study of emeraldine in salt form. Part II," *Journal of Raman Spectroscopy*, vol. 31, pp. 1041-1049, 2000.
- [19] G. M. Do Nascimento, T. B. Silva, P. Corio, and M. S. Dresselhaus, "Charge-transfer behavior of polyaniline single wall carbon nanotubes nanocomposites monitored by resonance Raman spectroscopy," *Journal of Raman Spectroscopy*, vol. 41, pp. 1587-1593, 2010.
- [20] X.-b. Yan, Z.-j. Han, Y. Yang, and B.-k. Tay, "Fabrication of carbon nanotube-polyaniline composites via electrostatic adsorption in aqueous colloids," *The Journal of Physical Chemistry C*, vol. 111, pp. 4125-4131, 2007.
- [21] R. V. Salvatierra, M. M. Oliveira, and A. J. Zarbin, "One-pot synthesis and processing of transparent, conducting, and freestanding carbon nanotubes/polyaniline composite films," *Chemistry of Materials*, vol. 22, pp. 5222-5234, 2010.
- [22] P. Liu, X. Wang, and H. Li, "Preparation of carboxylated carbon nanotubes/polypyrrole composite hollow microspheres via chemical oxidative interfacial polymerization and their electrochemical performance," *Synthetic Metals*, vol. 181, pp. 72-78, 2013.
- [23] Y. Li, H. Peng, G. Li, and K. Chen, "Synthesis and electrochemical performance of sandwich-like polyaniline / graphene composite nanosheets," *European Polymer Journal*, vol. 48, pp. 1406-1412, 2012.
- [24] M. V. Kulkarni and B. B. Kale, "Studies of conducting polyaniline (PANI) wrapped-multiwalled carbon nanotubes (MWCNTs) nanocomposite and its application for optical pH sensing," *Sensors and Actuators B: Chemical*, vol. 187, pp. 407-412, 2013.
- [25] A. K. Sharma, Y. Sharma, R. Malhotra, and J. Sharma, "Solvent tuned PANI-CNT composites as advanced electrode materials for supercapacitor application," *Advanced Materials Letters*, vol. 3, pp. 82-86, 2012.
- [26] S. Yadav, A. Kumar, and C. Pundir, "Amperometric creatinine biosensor based on covalently coimmobilized enzymes onto carboxylated multiwalled carbon nanotubes / polyaniline composite film," *Analytical biochemistry*, vol. 419, pp. 277-283, 2011.
- [27] S. Abdul Almohsin, Z. Li, M. Mohammed, K. Wu, and J. Cui, "Electrodeposited polyaniline/multi-walled carbon nanotube composites for solar cell applications," *Synthetic Metals*, vol. 162, pp. 931-935, 2012.
- [28] T.-M. Wu, H.-L. Chang, and Y.-W. Lin, "Synthesis and characterization of conductive polypyrrole/multi-walled carbon nanotubes composites with improved solubility and conductivity," *Composites Science and Technology*, vol. 69, pp. 639-644, 2009.
- [29] J.-E. Huang, X.-H. Li, J.-C. Xu, and H.-L. Li, "Well-dispersed single-walled carbon nanotube/polyaniline composite films," *Carbon*, vol. 41, pp. 2731-2736, 2003.
- [30] Y. Liu, H. Wang, J. Zhou, L. Bian, E. Zhu, J. Hai, *et al.*, "Graphene/polypyrrole intercalating nanocomposites as supercapacitors electrode," *Electrochimica Acta*, vol. 112, pp. 44-52, 2013.
- [31] W.-D. Zhang, H.-M. Xiao, and S.-Y. Fu, "Preparation and characterization of novel polypyrrole-nanotube/polyaniline free-standing composite films via facile solvent-evaporation method," *Composites science and technology*, vol. 72, pp. 1812-1817, 2012.
- [32] C. Lu and Y.-W. Mai, "Anomalous electrical conductivity and percolation in carbon nanotube composites," *Journal of Materials Science*, vol. 43, pp. 6012-6015, 2008.
- [33] A. Eken, E. Tozzi, D. Klingenberg, and W. Bauhofer, "A simulation study on the combined effects of nanotube shape and shear flow on the electrical percolation thresholds of carbon nanotube/polymer composites," *Journal of Applied Physics*, vol. 109, p. 084342, 2011.
- [34] X. Wu, S. Qi, J. He, and G. Duan, "High conductivity and low percolation threshold in polyaniline/graphite nanosheets composites," *Journal of materials science*, vol. 45, pp. 483-489, 2010.
- [35] I. D. Rosca and S. V. Hoa, "Highly conductive multiwall carbon nanotube and epoxy composites produced by three-roll milling," *Carbon*, vol. 47, pp. 1958-1968, 2009.